Silicon Uptake in Diatoms Revisited: A Model for Saturable and Nonsaturable Uptake Kinetics and the Role of Silicon Transporters[1][OA]

Kimberlee Thamatrakoln[2,3]* and Mark Hildebrand[2]

Marine Biology Research Division, Scripps Institution of Oceanography, La Jolla, California 92093–0202

The silicic acid uptake kinetics of diatoms were studied to provide a mechanistic explanation for previous work demonstrating both nonsaturable and Michaelis-Menten-type saturable uptake. Using $^{68}Ge(OH)_4$ as a radiotracer for $Si(OH)_4$, we showed a time-dependent transition from nonsaturable to saturable uptake kinetics in multiple diatom species. In cells grown under silicon (Si)-replete conditions, $Si(OH)_4$ uptake was initially nonsaturable but became saturable over time. Cells prestarved for Si for 24 h exhibited immediate saturable kinetics. Data suggest nonsaturability was due to surge uptake when intracellular Si pool capacity was high, and saturability occurred when equilibrium was achieved between pool capacity and cell wall silica incorporation. In *Thalassiosira pseudonana* at low $Si(OH)_4$ concentrations, uptake followed sigmoidal kinetics, indicating regulation by an allosteric mechanism. Competition of $Si(OH)_4$ uptake with $Ge(OH)_4$ suggested uptake at low $Si(OH)_4$ concentrations was mediated by Si transporters. At high $Si(OH)_4$, competition experiments and nonsaturability indicated uptake was not carrier mediated and occurred by diffusion. Zinc did not appear to be directly involved in $Si(OH)_4$ uptake, in contrast to a previous suggestion. A model for $Si(OH)_4$ uptake in diatoms is presented that proposes two control mechanisms: active transport by Si transporters at low $Si(OH)_4$ and diffusional transport controlled by the capacity of intracellular pools in relation to cell wall silica incorporation at high $Si(OH)_4$. The model integrates kinetic and equilibrium components of diatom $Si(OH)_4$ uptake and consistently explains results in this and previous investigations.

For decades, models of Michaelis-Menten-type saturable kinetics of nutrient uptake and assimilation in phytoplankton have guided our understanding of how the cell translates nutrient availability into growth (Eppley et al., 1969; Sullivan, 1976, 1977; McCarthy, 1981; Del Amo and Brzezinski, 1999). However, several studies suggest uptake, under certain conditions, is nonsaturable and in some cases biphasic (Wheeler et al., 1982; Collos et al., 1992; Watt et al., 1992; Collos et al., 1997; Lomas and Glibert, 1999). Conclusions regarding uptake kinetics of nutrients have been variable, due in part to differences in the methods applied, making comparison of data difficult. Factors contributing to these variations include species-specific or cell size differences, the physiological state of cultures, and the incubation period and nutrient concentration range over which uptake is measured (Sullivan, 1976; Wheeler et al., 1982; Harrison et al., 1989; Collos et al., 1992; Lomas and Glibert, 1999; Leynaert et al., 2004). The attractive simplicity of a Michaelis-Menten kinetic model for uptake (control by the transporter itself, similar to an enzymatic process) in some cases may have precluded efforts to explain factors involved in biphasic or nonsaturable kinetics. However, transporters do not convert their substrate into a product but rather are involved in generating what is oftentimes a nonequilibrium gradient of the molecule across a lipid bilayer. Thus, other factors involved in generating and maintaining the state of equilibrium will influence kinetic properties of transport.

Diatoms are one of the largest groups of silicifying organisms, and most species have an obligate requirement for silicon (Si) for cell wall formation. Si transporters, or SITs, are specific membrane-associated proteins shown to transport $Si(OH)_4$ across lipid bilayer membranes (Hildebrand et al., 1997, 1998). SITs have been identified in numerous diatom species (Grachev et al., 2002; Sherbakova et al., 2005; Thamatrakoln et al., 2006) as well as in the Chrysophytes *Synura petersenii* and *Ochromonas ovalis* (Likoshway et al., 2006). SITs have also been identified in plants, but these proteins are homologous to plant aquaporins or bacterial arsenic effluxers and share no similarity with diatom SITs (Ma et al., 2004; Ma et al., 2007). Mechanistic models for Si transport in diatoms have recently been proposed (Sherbakova et al., 2005; Thamatrakoln et al., 2006), including one (Sherbakova et al., 2005) with a hypothesis for the proposed involvement of zinc in $Si(OH)_4$ uptake (Rueter and Morel, 1981).

In diatoms, $Si(OH)_4$ uptake has been typically characterized by Michaelis-Menten-type saturation kinet-

[1] This work was supported by the Air Force Office of Scientific Research Multidisciplinary University Research Initiative (grant no. RF00965521 to M.H.).

[2] These authors contributed equally to the article.

[3] Present address: Institute of Marine and Coastal Sciences, Rutgers University, 71 Dudley Road, New Brunswick, NJ 08901.

* Corresponding author; e-mail thamat@marine.rutgers.edu.

The author responsible for distribution of materials integral to the findings presented in this article in accordance with the policy described in the Instructions for Authors (www.plantphysiol.org) is: Kimberlee Thamatrakoln (thamat@marine.rutgers.edu).

[OA] Open Access articles can be viewed online without a subscription.
www.plantphysiol.org/cgi/doi/10.1104/pp.107.107094

ics, although nonsaturable and biphasic kinetics have occasionally been observed (Table I). Many kinetics studies on diatom $Si(OH)_4$ uptake utilized long-term incubations; however, it is well established that intrinsic kinetic properties need to be measured in the short term prior to the influence of equilibrium effects. Equilibrium factors influencing $Si(OH)_4$ uptake in diatoms include low extracellular $Si(OH)_4$ concentrations (<100 μM; Tréguer et al., 1995; Martin-Jézéquel et al., 2000); high intracellular concentrations (up to hundreds of millimolars); and different forms of Si, extracellular being silicic acid or silicate, intracellular thought to consist of silicic acid complexed with organics (Azam et al., 1974; Sullivan, 1979), and the solid form of silica in the cell wall (Martin-Jézéquel et al., 2000). Unlike other nutrients, silicic acid has a unique chemistry in that it autopolymerizes into silica at concentrations >2 mM at neutral pH (Iler, 1979), but intracellular pools in diatoms have been measured well above silica saturation (19–340 mM; Martin-Jézéquel et al., 2000). Electron spectroscopic imaging indicates intracellular Si is not sequestered in vesicles (Rogerson et al., 1987), and other data suggest that maintenance of supersaturated levels of silicic acid is likely through an association of intracellular Si with as-yet-uncharacterized organic components (Azam et al., 1974; Sullivan, 1979; Hildebrand, 2000; Hildebrand and Wetherbee, 2003). The balance between these binding components and free $Si(OH)_4$ will also influence the equilibrium state of $Si(OH)_4$. Si efflux is an often overlooked and under-

Table I. *Previously published studies on $Si(OH)_4$ uptake in diatoms*

Listed are species used in the study, whether cultures were prestarved for Si prior to measuring uptake, the incubation period, $Si(OH)_4$ concentrations over which uptake was measured, the method, the results, and the reference.

Species	Prestarved?	Incubation Period	$Si(OH)_4$	Method	Results	Reference
			$\mu mol\ L^{-1}$			
T. pseudonana clone 3H	No	>1 h	0–14	Silico-molybdate	Michaelis-Menten hyperbola	Paasche (1973a)
Skeletonema costatum *T. pseudonana* *Thalassiosira decipiens* *Ditylum brightwellii* *Licmophora* sp.	Yes	1 h	0–15	Silico-molybdate	Michaelis-Menten hyperbola	Paasche (1973b)
N. alba	Yes	<10 min	0–20	^{31}Si	Michaelis-Menten hyperbola	Azam et al. (1974)
N. alba	Yes	15 s–3 min	0–80	^{68}Ge	Michaelis-Menten hyperbola	Azam (1974)
N. alba	Yes	<2 min	0–32	^{68}Ge	Biphasic	Azam and Volcani (1974)
T. pseudonana Clone 3H Clone 13-1	Both Si replete and prestarved	4 h	0–15	^{30}Si	Clone 3H Replete: nonsaturable Prestarved: Michaelis-Menten hyperbola Clone 13-1 Replete and prestarved: Michaelis-Menten hyperbola	Nelson et al. (1976)
N. pelliculosa FW	Yes	2 min	0–100	^{68}Ge	Michaelis-Menten hyperbola	Sullivan (1976)
P. tricornutum	Yes	2 h	Up to 160 μM	^{30}Si	Michaelis-Menten hyperbola	Reidel and Nelson (1985)
T. pseudonana *T. weissflogii* *C. fusiformis* *P. tricornutum*	Yes	3–4 h	0–35 or 0–300	^{32}Si	*T. pseudonana*, *T. weissflogii*, and *C. fusiformis*: Michaelis-Menten hyperbola *P. tricornutum*: Michaelis-Menten hyperbola at 0–25 μM $Si(OH)_4$, nonsaturable at 25–300 μM $Si(OH)_4$	Del Amo and Brzezinski (1999)
C. fusiformis	No	4 h	0–15	^{32}Si	Michaelis-Menten hyperbola	Leynaert et al. (2004)
T. weissflogii	No	1 h	0–30	^{32}Si	Michaelis-Menten hyperbola	Milligan et al. (2004)

appreciated aspect of balancing the overall cellular Si budget, with net uptake involving both uptake and efflux (Azam et al., 1974; Sullivan, 1976; Milligan et al., 2004).

A model for Si transport in diatoms suggests uptake is controlled by the rate of cell wall silica incorporation through the intermediary of intracellular soluble Si pools (Conway et al., 1976; Conway and Harrison, 1977; Hildebrand, 2000; Hildebrand and Wetherbee, 2003). Three modes of Si uptake in diatoms, surge uptake, externally controlled uptake, and internally controlled uptake, have been defined from chemostat experiments (Conway et al., 1976; Conway and Harrison, 1977). Surge uptake occurs upon initial addition of Si to Si-starved cells, with maximal uptake rates occurring at this time. Externally controlled uptake is dictated by external Si concentrations. In internally controlled uptake, rates are regulated by the rate of cell wall silica incorporation (Conway and Harrison, 1977).

The described model for Si transport deals mainly with equilibrium processes and does not completely explain observed kinetic parameters (Table I). In each study (Table I) documenting Michaelis-Menten-type saturation kinetics for $Si(OH)_4$ uptake in diatoms, either (1) cultures were maintained in Si-free medium for an extensive period of time (24 h) prior to measuring uptake; (2) uptake was measured over long (hours) incubation times; or (3) low $Si(OH)_4$ concentrations were used (Table I). When these conditions were not followed, nonsaturable uptake kinetics were observed (Table I), but explanations for nonsaturable kinetics have not been provided.

To correlate kinetic observations with equilibrium processes in the model for $Si(OH)_4$ transport, we measured both short-term (minutes) and long-term (hours) uptake in different diatom species using the radiotracer analog of silicic acid, $^{68}Ge(OH)_4$. In addition, we determined and could control conditions to produce saturable or nonsaturable $Si(OH)_4$ uptake kinetics. Based on these data and previous studies, a revised model of $Si(OH)_4$ uptake in diatoms, in which both carrier-mediated and diffusional transport occurs, was developed to provide explanations for observed kinetics curves based on equilibrium factors.

RESULTS

$Si(OH)_4$ Uptake in *Thalassiosira pseudonana* Transitioned from Nonsaturable to Saturable Kinetics over Time

In previous work, incubation time was one variable distinguishing Michaelis-Menten saturating from nonsaturating or biphasic $Si(OH)_4$ uptake kinetics in diatoms (Table I). To determine the effect of incubation time on $Si(OH)_4$ uptake kinetics, uptake rates were measured on the same sample of exponentially growing *T. pseudonana* by incubation with various silicate concentrations and removing aliquots to measure uptake after 2 min, 10 min, 30 min, 1 h, 2 h, and 3 h. In Figure 1, curves were fit by nonlinear regression using Michaelis-Menten hyperbolas. Kinetic parameters are listed in Table II. For $Si(OH)_4$ uptake after 2 and 10 min, a Michaelis-Menten hyperbola could be fit to the data, but a clear plateau was not observed and uptake appeared nonsaturable. In addition, the 95% confidence intervals for K_s [the half-saturation constant defined as the $Si(OH)_4$ concentration at 0.5 V_{max}] and V_{max} were extremely wide, suggesting a poor fit of the data to a Michaelis-Menten model (Table II). In a separate experiment, short-term uptake continued to increase at concentrations up to 500 μmol L^{-1}, and data could not be fit to a Michaelis-Menten hyperbola (data did not converge) consistent with uptake being nonsaturable (Fig. 1, 2-min inset). Comparing Michaelis-Menten plots from 30 min to 3 h, the curves gradually sloped over, and saturation was observed between 1 and 2 h (Fig. 1). Based on measurements of Si requirements for the cell wall of *T. pseudonana* (Hildebrand et al., 2007), $Si(OH)_4$ would not be depleted in the long-term incubations, indicating that sloping over was not due to a transition to externally controlled uptake.

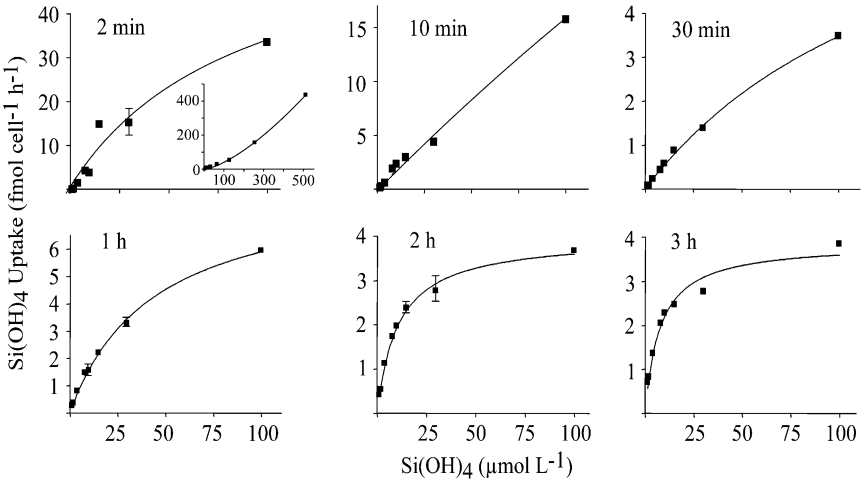

Figure 1. Effect of incubation time on $Si(OH)_4$ uptake kinetics in *T. pseudonana*. Uptake rates were measured in cells incubated in various silicate concentrations for 2 min, 10 min, 30 min, 1 h, 2 h, or 3 h. Curves represent fitted Michaelis-Menten hyperbolas obtained by nonlinear regression. For 8 to 30 μmol L^{-1} $Si(OH)_4$ concentrations, the average of duplicates is plotted. Error bars are SE. Inset graph in 2-min uptake represents $Si(OH)_4$ uptake at concentrations up to 500 μmol L^{-1}. To compare rates between experiments and with past data, all uptake rates were expressed in hours even when short-term (e.g. minutes) uptake was measured.

Table II. *Kinetic parameters of $Si(OH)_4$ uptake in T. pseudonana*

Half-saturation constant, K_s, and V_{max} values are shown, with 95% confidence limits shown in parentheses. R^2 values represent goodness of fit for Michaelis-Menten hyperbolas.

Incubation Time	K_s	V_{max}	R^2
h	*μmol L⁻¹*	*fmol cell⁻¹ h⁻¹*	
0.03	78.43 (±71.68)	59.99 (±33.79)	0.9033
0.166	868.1 (±1,814.2)	151.5 (±289.85)	0.9842
0.5	149.6 (±42.5)	21.65 (±4.31)	0.9956
1	43.63 (±9.28)	8.43 (±0.982)	0.9896
2	10.32 (±2.86)	3.92 (±0.408)	0.9728
3	7.04 (±2.16)	3.73 (±0.374)	0.9617

Biphasic Uptake Kinetics in *T. pseudonana*

Previous experiments in *T. pseudonana* reported saturation at $Si(OH)_4$ concentrations <50 μmol L^{-1} (Table I), in contrast to our results (Fig. 1, 2-min inset). To address this, uptake at $Si(OH)_4$ concentrations between 1 and 100 μmol L^{-1} was analyzed in more detail on multiple biological and technical replicates (n = 11). Biphasic kinetics were observed, with a nonsaturable aspect above 30 μmol L^{-1} (Fig. 2A, inset) and a sigmoidal dose-response curve (a Michaelis-Menten hyperbola resulted in a poor fit of the data) below 30 μmol L^{-1} (Fig. 2A), with $K_{0.5}$ = 8.1 ± 1.4 μmol L^{-1} and V_{max} = 8.4 ± 1.1 fmol $cell^{-1}$ h^{-1}. The Hill slope, an indicator of the degree of cooperativity (Koshland et al., 1966), was 2.7, suggesting a positively cooperative uptake system. To investigate this in more detail, short-term uptake was measured (n = 7) for $Si(OH)_4$ concentrations <30 μmol L^{-1}, at every 2 μmol L^{-1}. Data were fit to either a Michaelis-Menten hyperbola or a sigmoidal dose-response curve, with the latter curve (Fig. 2B) producing the better fit, with $K_{0.5}$ = 8.0 ± 0.94 μmol L^{-1}, V_{max} = 32.6 ± 2.8 fmol $cell^{-1}$ h^{-1}, and a Hill slope of 1.9. Long-term uptake kinetics <30 μmol L^{-1} were also analyzed; in individual experiments at 2 and 3 h, uptake also showed sigmoidal kinetics (Fig. 2C), with $K_{0.5}$ = 7.2 μmol L^{-1} and 5.6 μmol L^{-1}, respectively.

SITs Mediate Uptake at Low $Si(OH)_4$ Concentrations

To determine the role SITs played in uptake at different concentrations of $Si(OH)_4$, we tested potential inhibitors of SITs. Zinc has been proposed to be an essential component of Si transport (Rueter and Morel, 1981) by binding to a functional site on SITs and facilitating the formation of a ternary complex with silicic acid (Sherbakova et al., 2005). The effect of removing zinc on $Si(OH)_4$ uptake was investigated using two chelators: membrane-impermeable Na_2EDTA and zinc-specific, membrane-permeable *N*,*N*,*N*′,*N*-tetrakis(2-pyridylmethyl)ethylenediamine (TPEN). Chelators used at 10-fold molar excess to zinc inhibited growth (data not shown). Growth of TPEN-inhibited cultures could be rescued by the addition of zinc but not by the addition of calcium or iron, suggesting TPEN was specifically removing zinc from the medium (Fig. 3A, inset). Chelators had no effect on $Si(OH)_4$ uptake rates (Fig. 3A), suggesting removal of zinc could not be used as a SIT inhibitor. Data obtained by Rueter and Morel (1981) suggesting that zinc was involved in uptake resulted from a long-term incubation experiment, suggesting secondary effects on cellular metabolism could have resulted in their observed inhibition of uptake.

Germanic acid, or $Ge(OH)_4$, is a competitive inhibitor of $Si(OH)_4$ uptake (Azam et al., 1974), indicating an interaction at the $Si(OH)_4$ binding site. Short-term uptake was monitored in cells treated with different concentrations but a constant ratio (1:0.33) of $Si(OH)_4$: unlabeled $Ge(OH)_4$. Similar to untreated cells, a biphasic curve was seen in $Ge(OH)_4$-treated cells (Fig. 3B). However, between 4 and 30 μmol L^{-1}, uptake became

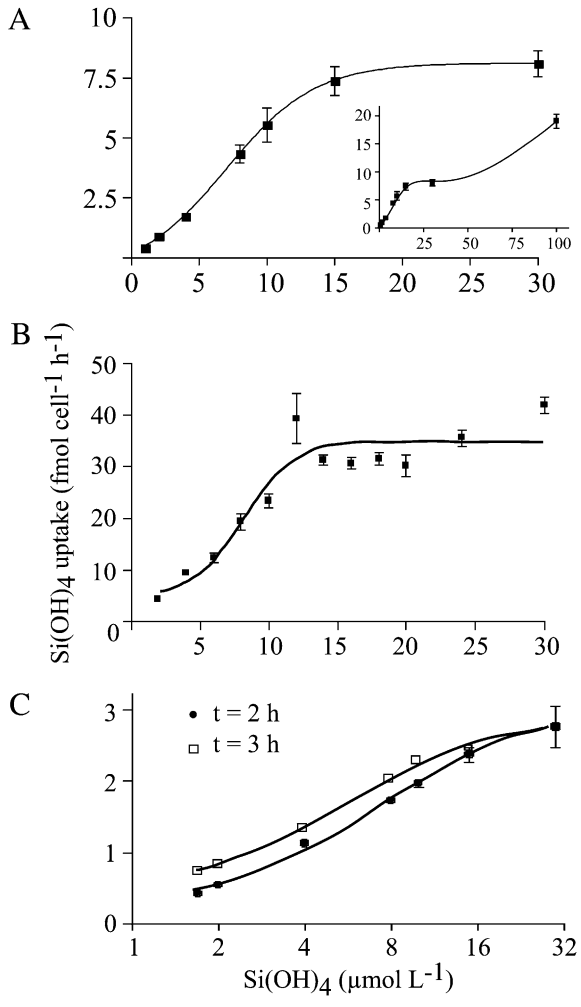

Figure 2. Detailed analysis of $Si(OH)_4$ uptake. Data were fit by nonlinear regression using a sigmoidal dose-response model. The mean with SE is shown. A, Short-term (2 min) uptake at 1 to 30 μmol L^{-1} $Si(OH)_4$. Inset shows uptake up to 100 μmol L^{-1} (n = 11). B, Short-term uptake measured every 2 μmol L^{-1} $Si(OH)_4$ up to 30 μmol L^{-1} (n = 7). C, Long-term uptake (2 and 3 h) below 30 μmol L^{-1}.

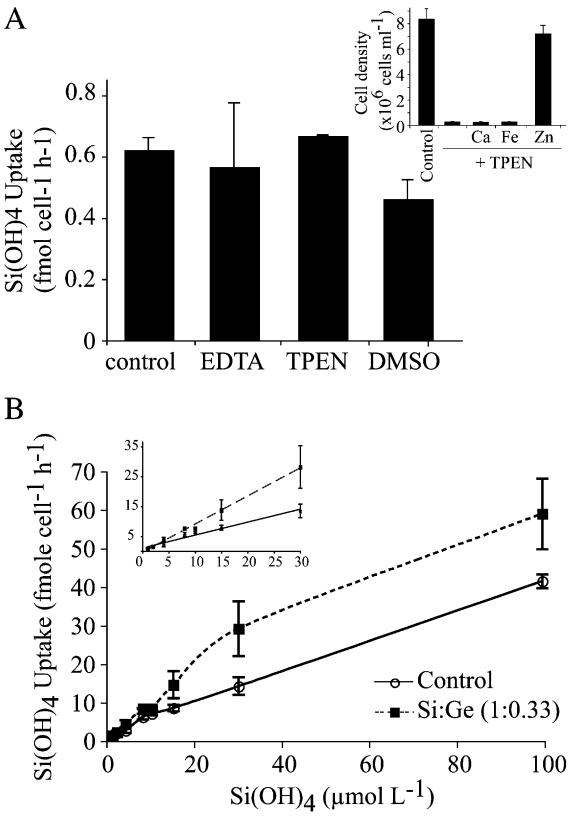

Figure 3. A, Effect of zinc chelators on $Si(OH)_4$ uptake. Membrane-permeable chelator TPEN and membrane-impermeable chelator Na_2EDTA were added to cells at 50 μmol L^{-1}. $Si(OH)_4$ uptake in 15 μmol L^{-1} $Si(OH)_4$ was monitored after 30 min. Control cells had no addition, and another control had an equal volume of DMSO as used for the TPEN solution. The mean of triplicate measurements is shown along with SE. Cell density was monitored in cultures grown in ASW (control) or ASW + TPEN after the addition of Ca, Fe, or Zn (inset). The mean of duplicates is shown with SD. B, Comparison of short-term (2 min) $Si(OH)_4$ uptake using the standard protocol (white circles, solid line) and with a constant ratio of unlabeled $Si(OH)_4$ to $Ge(OH)_4$ (black squares, dashed line). Inset shows the slope of both conditions between 1 and 30 μmol L^{-1}; slope above 30 μmol L^{-1} is evident in the original plot.

increasingly greater in treated cells (Fig. 3B, inset) in contrast to uptake at $Si(OH)_4$ concentrations >30 μmol L^{-1}, which increased proportionally in the control and $Ge(OH)_4$-treated cells (Fig. 3B). The effect of $Ge(OH)_4$ on transport at low $Si(OH)_4$ suggested this portion of the curve involved SITs, whereas the lack of an effect at high $Si(OH)_4$ supports data in Figure 1 (2-min inset) that suggests diffusional transport dominated at these concentrations.

Uptake Kinetics in *Navicula pelliculosa* FW and the Effect of Si Starvation

Another variable distinguishing Michaelis-Menten-type saturating from nonsaturating or biphasic $Si(OH)_4$ uptake kinetics in previous work was whether or not cells were prestarved for Si for a long time period (Table I). To test if nonsaturability of short-term $Si(OH)_4$ uptake (Figs. 1 and 2A) observed in *T. pseudonana* was due to experimental design (e.g. lack of extensive prestarvation) or whether species-specific effects were involved, $Si(OH)_4$ uptake was monitored in *N. pelliculosa* FW where short-term uptake (2 min) was previously shown to be saturable (Sullivan, 1976, 1977). To compare the effect of experimental design, $Si(OH)_4$ uptake was measured using both the current method (exponentially growing cells with a 5- to 10-min incubation in Si-free medium) as well as Sullivan's method (incubation of exponentially growing cells in Si-free medium for 24 h). Using the same method used in Figures 1 and 2 for *T. pseudonana*, $Si(OH)_4$ uptake was measured in *N. pelliculosa* FW after 2 and 30 min. For 2-min uptake, a Michaelis-Menten hyperbola resulted in a poor fit of the data (r^2 = 0.8557), indicating nonsaturable kinetics (Fig. 4A, left). Uptake after 30 min fit a Michaelis-Menten saturating hyperbola (r^2 = 0.9968) with K_s = 48.5 μmol L^{-1} and V_{max} = 5.0 fmol $cell^{-1}$ h^{-1} (Fig. 4A, right). Thus, a transition from nonsaturable to saturable kinetics occurred with increasing incubation time in exponentially grown *N. pelliculosa* FW, as with *T. pseudonana*. When cultures of *N. pelliculosa* FW were maintained in Si-free medium for 24 h (long-term Si starvation), short-term (2 min) uptake saturated immediately (K_s = 14.3 μmol L^{-1} and

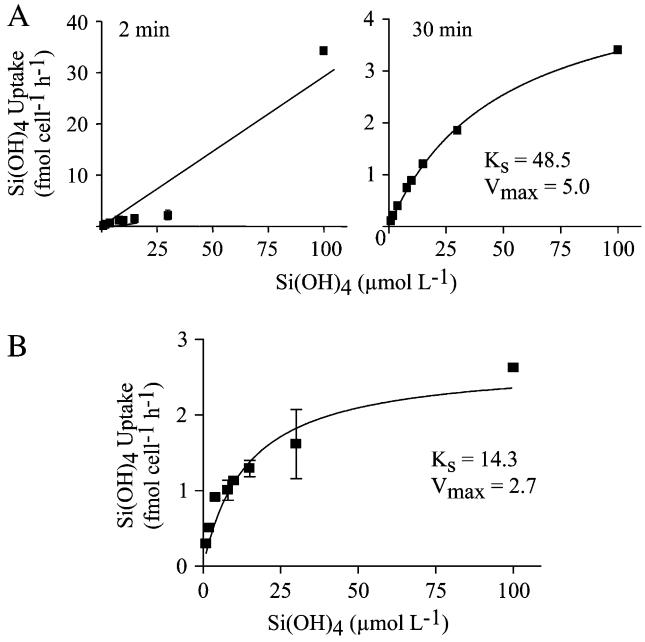

Figure 4. $Si(OH)_4$ uptake kinetics of *N. pelliculosa* FW. All data were fit by nonlinear regression using Michaelis-Menten hyperbolas. A, Left graph shows short-term (2 min) uptake kinetics using the same method used for *T. pseudonana* in Figures 1 and 2. Right graph is uptake kinetics for the same cells measured after 30 min. B, In contrast, cells here were maintained in Si-free medium for 24 h prior to measuring short-term uptake kinetics (2 min). Error bars for 8 to 30 μmol L^{-1} $Si(OH)_4$ concentrations are SE of two replicates. Values for K_s (in micromoles per liter) and V_{max} (in femtomoles per cell per hour) were calculated using GraphPad Prism 4.

V_{max} = 2.7 fmol cell^{-1} h^{-1}; Fig. 4B) as previously observed (Sullivan, 1976, 1977). Short-term uptake in *T. pseudonana* after 24 h in Si-free medium also showed Michaelis-Menten-type saturation kinetics (data not shown), confirming this was not a species-specific effect.

Intracellular Pool Capacity and Levels Differ under Different Growth Conditions

Because intracellular soluble Si pool levels decrease during Si starvation (Martin-Jézéquel et al., 2000), data in Figure 4 suggested the status of intracellular pools was involved in the transition from nonsaturable to saturable kinetics. In a representative experiment in *T. pseudonana* (Fig. 5A), pool levels were relatively low during exponential growth, but after 5 to 10 min in Si-free medium (as was done for the kinetics measurements), levels increased substantially within 5 min after $Si(OH)_4$ addition, consistent with surge uptake measured in kinetics experiments (Figs. 1 and 2A). Pools then gradually decreased (Fig. 5A). Comparison of intracellular pools (Fig. 5B) in multiple exponentially growing cultures showed relatively low levels of $Si(OH)_4$ (average 5.35 fmol cell^{-1}), even in cases where extracellular $Si(OH)_4$ concentrations were far higher than 100 μmol L^{-1} when surge uptake occurred after processing for kinetics measurements (Fig. 5A). Thus, surge uptake was prevented under conditions of exponential growth.

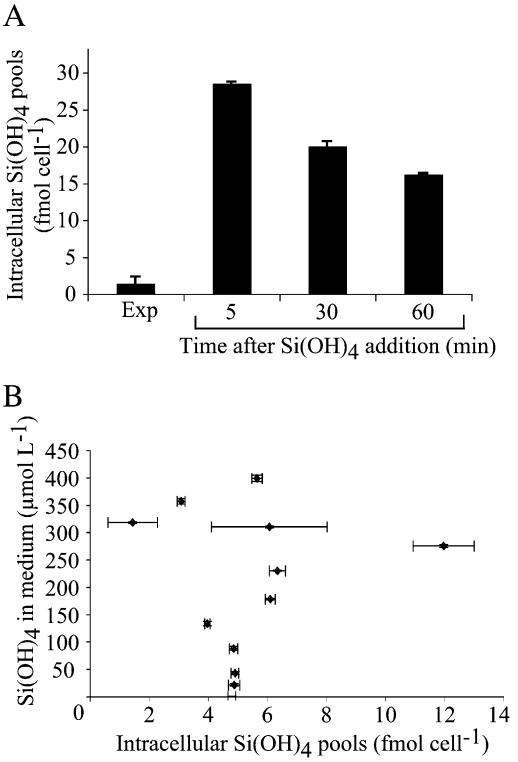

Figure 5. Measurement of intracellular $Si(OH)_4$ pools under different growth conditions. A, Pools were measured in exponentially growing (Exp) cells and then over time in cells spiked with 100 μmol L^{-1} $Si(OH)_4$ after a brief Si starvation (5–10 min). The mean of duplicate measurements is shown with SE. B, Pools measured in exponentially growing cultures (n = 13) compared to $Si(OH)_4$ levels in the medium. The mean of duplicate measurements is shown with SE.

Comparison of Uptake Characteristics in Different Diatom Species

A survey of different diatom species was done to determine how common nonsaturable $Si(OH)_4$ uptake on short time scales was and whether uptake saturated on longer time scales. $Si(OH)_4$ uptake was measured in different diatom species using the same method as for *T. pseudonana* in Figure 1. For each species tested, full kinetic curves were obtained for each incubation period, but for simplicity only V_{max} at the highest tested $Si(OH)_4$ concentration for each incubation period is shown in Figure 6A. In each species, short-term (2 min) $Si(OH)_4$ uptake was maximal and nonsaturable and decreased with increased time (Fig. 6A). For short-term uptake, *Thalassiosira weissflogii* had the highest V_{max}, while *N. pelliculosa* M had the lowest. Saturation was achieved in all species except *T. weissflogii* (which tended toward saturation but did not achieve it). The time required to achieve saturation varied. The percentage of uptake over time relative to the maximum at 2 min (Fig. 6B) was plotted, and exponential decay curves were used to calculate when saturation (defined as 15% of the 2-min value based on the appearance of the curve) was achieved. *N. pelliculosa* FW (4.8-min saturation time), *Chaetoceros gracilis* (10.8 min), and *N. pelliculosa* M (13.8 min) saturated earlier than the others, with *T. pseudonana* (43.3 min) taking the longest to saturate.

Comparison of Cell Wall Silica to Intracellular Pool Size in Different Diatom Species

Because cell wall silica incorporation can be a controlling factor over uptake through the intermediary of intracellular pools (Conway et al., 1976; Conway and Harrison, 1977; Hildebrand, 2000; Hildebrand and Wetherbee, 2003), intracellular soluble Si pool concentrations and the amount of cell wall silica were measured in each species during exponential growth to determine whether these parameters were related to the rate at which saturation was achieved. The ratio of cell wall silica to soluble intracellular pools is shown in Figure 7. Although there was no consistent relationship between this ratio and the rate of saturation, selected examples will be discussed below.

DISCUSSION

The goal of this study was to provide mechanistic explanations for saturable versus nonsaturable kinetics of $Si(OH)_4$ uptake previously described in diatoms (Table I). We determined, and could control, specific

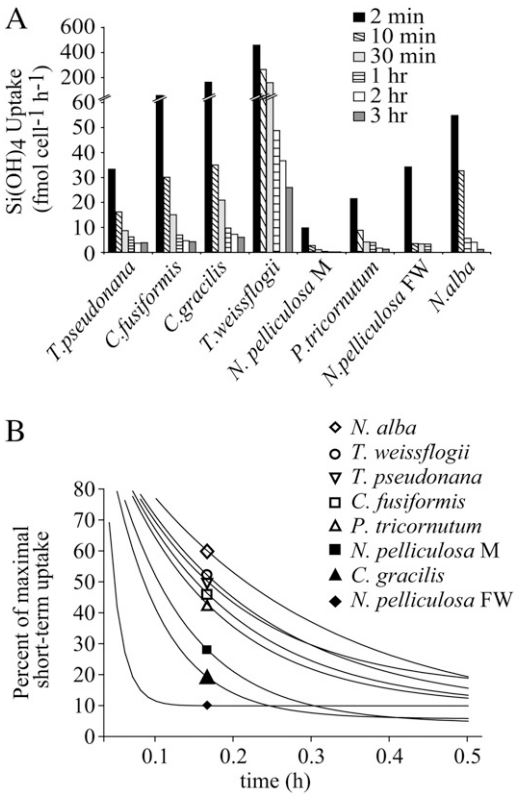

Figure 6. Maximum $Si(OH)_4$ uptake rates and time to achieve saturable kinetics for different diatom species. A, Maximum rate of $Si(OH)_4$ uptake for different diatom species after 2 min, 10 min, 30 min, 1 h, 2 h, or 3 h. *T. pseudonana*, *C. fusiformis*, *C. gracilis*, *P. tricornutum*, and *N. pelliculosa* FW were incubated with 100 μmol L^{-1} $Si(OH)_4$. *T. weissflogii*, *N. pelliculosa* M, and *N. alba* were incubated with 30 μmol L^{-1} $Si(OH)_4$. Break in *y* axis is shown. B, Rate of decrease in uptake for different species based on percent of maximal uptake at 2 min over time. Exponential decay curves were fit; symbols denote the different species.

conditions producing saturable and nonsaturable $Si(OH)_4$ uptake in multiple diatom species. Long-term (24 h) Si-starved cells demonstrated saturable kinetics (Fig. 4B), whereas cells only briefly (5–10 min) Si starved showed nonsaturable uptake kinetics (Figs. 1, 4A, and 6). In these cells, nonsaturable kinetics transitioned to saturable kinetics over time (Figs. 1, 4A, and 6), which occurred primarily because of equilibration between intracellular soluble Si pool capacity and cell wall silica incorporation. Uptake at low $Si(OH)_4$ concentrations was saturable and mediated by SITs, while uptake at high $Si(OH)_4$ was nonsaturable and occurred by diffusion (Figs. 1 and 3). Based on these data, a revised model of $Si(OH)_4$ uptake was developed in which equilibrium factors were used to explain kinetics curves resulting from these conditions.

$Si(OH)_4$ Uptake in *T. pseudonana* Occurs through Two Distinct Mechanisms

At $Si(OH)_4$ concentrations <30 μmol L^{-1} in both short-term and long-term uptake, SITs controlled uptake, resulting in sigmoidal kinetics. Sigmoidal kinetics are diagnostic of allosteric cooperative interactions (e.g. homo- or heterodimers) and have been described for both enzymes and transporters (Hamill et al., 1999; Zelcer et al., 2003; Higgins and Linton, 2004; Suana and Ambudkar, 2007). The Hill coefficient estimates the minimal number of interacting binding sites in a positively cooperating system and suggests here that $Si(OH)_4$ uptake involves at least two and perhaps three binding events (Hill coefficients = 1.9–2.7). This could indicate sequential $Si(OH)_4$ binding or, because SITs are sodium symporters (Bhattacharyya and Volcani, 1983; Hildebrand, 2000), could indicate sequential sodium and $Si(OH)_4$ binding. Another type of allosteric mechanism that could explain sigmoidal kinetics is the alternating access model for transmembrane transport, where specific conformational changes promote binding at one site and affect binding at another. This mechanism has been proposed for SITs (Thamatrakoln et al., 2006) and could contribute to the allostery seen in Figure 2. Although our current data do not allow determination of the degree to which the different mechanisms described may contribute to sigmoidal kinetics, allostery may explain why the competitive inhibitor $Ge(OH)_4$ (Azam et al., 1974) stimulated uptake at low $Si(OH)_4$ concentrations (Fig. 3B). Allosteric uptake mechanisms can stimulate uptake with increasing amounts of substrate, even if substrates are competing for the same binding site.

The positive degree of cooperativity with increasing $Si(OH)_4$ (Fig. 2) altered SIT activity depending on extracellular $Si(OH)_4$ concentrations in a nonlinear way. One consequence is that SITs may limit uptake at suboptimal $Si(OH)_4$ concentrations, for example, if extracellular $Si(OH)_4$ concentrations are too low to provide sufficient precursor to complete cell wall synthesis. Darley and Volcani (1969) showed in *Cylindrotheca fusiformis* that a threshold level of $Si(OH)_4$ was

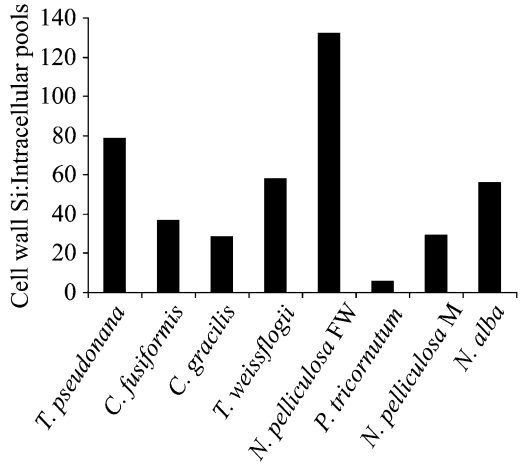

Figure 7. Ratio of cell wall silica to intracellular soluble Si pools for exponentially growing diatom species used in this study. See "Materials and Methods" for experimental details.

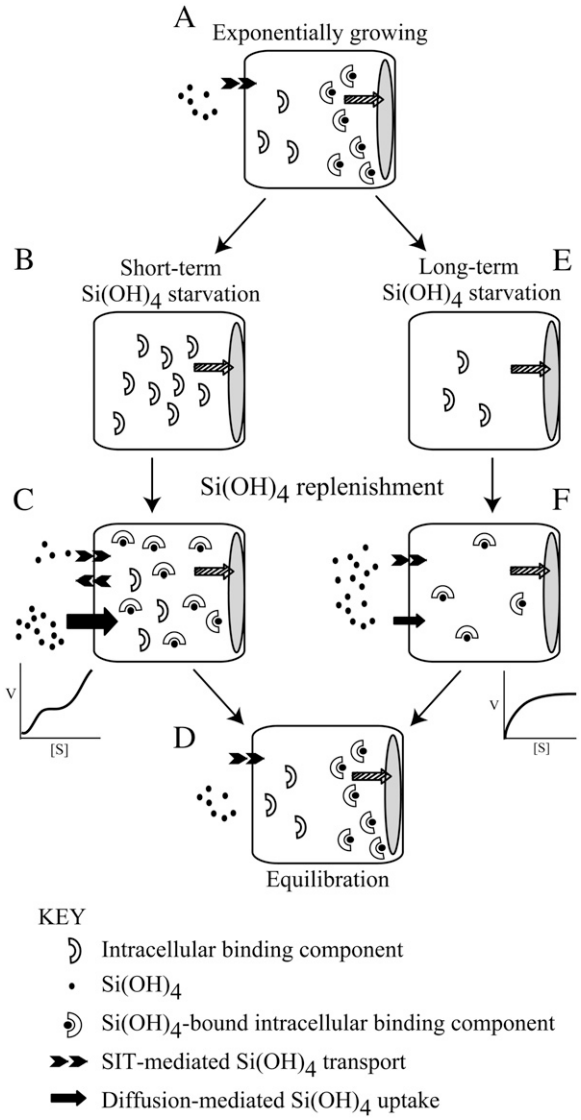

Figure 8. Proposed model of Si uptake in diatoms. In each image, a diatom cell is represented as a rectangular box and cell wall silica (i.e. the silica deposition vesicle, SDV) is represented as a gray elongated oval. Black dots represent $Si(OH)_4$. Horseshoe-shaped structures represent intracellular Si-binding components that data suggest are present but have yet to be identified. Arrows denote direction of transport with magnitude indicated by their thickness. Black arrows denote diffusion-mediated uptake, and broken arrows represent SIT-mediated transport. Hatched arrows show movement of $Si(OH)_4$ into the SDV. Stylized graphs of uptake kinetics are shown for C and E. A, In exponentially growing cells, equilibration is achieved between uptake rate, intracellular pools, and cell wall silica incorporation. Uptake is internally controlled. B, After a brief (5–10 min) incubation in Si-free medium, levels of intracellular-binding component have delivered $Si(OH)_4$ to the SDV and are predominantly in the uncomplexed state. C, Upon $Si(OH)_4$ replenishment, cells are able to accommodate surge uptake mediated by diffusion at high $Si(OH)_4$, and nonsaturable uptake kinetics are observed. Biphasic curves are seen because, at low $Si(OH)_4$ concentrations, SITs are still capable of mediating uptake. In *T. pseudonana*, this results in sigmoidal kinetics. SIT-mediated efflux aids in equilibration. D, After time (approximately 1 h in *T. pseudonana*), equilibration is re-established between the level of binding component and the rate of silica incorporation, and uptake becomes internally controlled. E, During long-term (24 h) Si starvation, the level of binding component becomes reduced. F, Upon $Si(OH)_4$ replenishment, intracellular capacity is low, and cells are not able to accommodate surge uptake; thus, Michaelis-Menten type saturation is observed.

required to stimulate DNA replication and cytokinesis, consistent with this hypothesis.

Uptake $>30\ \mu mol\ L^{-1}$ $Si(OH)_4$ was nonsaturable (Fig. 1, 2-min inset) and likely mediated by simple diffusion, as opposed to facilitated diffusion (i.e. uptake through a carrier), which would be expected to saturate due to limitations in the numbers of carriers. This is supported by the lack of an effect of adding extra unlabeled $Ge(OH)_4$ (Fig. 3B) where the slopes of the curves $>30\ \mu mol\ L^{-1}$ were nearly identical. Recently, it was proposed that $Si(OH)_4$ uptake in diatoms could occur by pinocytosis (Vrieling et al., 2007); however, pinocytosis is a saturable process, which is inconsistent with our data. Diffusion of $Si(OH)_4$, which has been previously shown to occur across a membrane (Johnson and Volcani, 1978), may seem counterintuitive in a diatom cell because intracellular concentrations are far higher than extracellular levels. However, if intracellular Si is bound by organic compounds, the chemical form is different and an inward concentration gradient for $Si(OH)_4$ would exist.

A Revised Model for $Si(OH)_4$ Uptake in Diatoms

Examination of the kinetic response to short- and long-term Si starvation (Figs. 1 and 4), and measurements of intracellular pools (Fig. 5), indicates a major controlling factor regulating the transition from nonsaturable to saturable uptake is the capacity of intracellular pools to accommodate excess soluble Si. Based on this, we propose the following model to explain the kinetic properties of diatom $Si(OH)_4$ uptake (Fig. 8). In exponentially growing cultures, intracellular $Si(OH)_4$ levels are relatively low, but the capacity of pools is high (Fig. 5). We propose that during the brief period (5–10 min) of Si starvation prior to the measurement of uptake, intracellular binding components continue to release their Si for incorporation, but because no extracellular Si is present, they are not recharged (Fig. 8B). Thus, when cells are subsequently incubated with $Si(OH)_4$, the binding capacity of pools is high, and a nonsaturable surge occurs (Fig. 8C). Higher V_{max} values measured at 2, 10, and 30 min versus those at 2 and 3 h (Fig. 1; Table II) suggests that over time, nonsaturable uptake transitions to saturable uptake because equilibrium is achieved between the capacity of binding components and their delivery rate of Si to the cell wall (Fig. 8D); thus, the rate of uptake becomes controlled by the rate of cell wall silica incorporation (i.e. internally controlled uptake). In extensively (24 h) Si-starved cultures of *T. pseudonana* (Fig. 8, E and F), pools also increase rapidly upon $Si(OH)_4$ addition but not to the extent seen in Figure 5A, and rather than

decrease over time, they gradually increase (Hildebrand et al., 2007). Pool levels are minimal after prolonged Si starvation (Martin-Jézéquel et al., 2000); thus, we propose that levels of soluble Si-binding component decrease (Fig. 8E), and the diminished intracellular capacity results in saturable kinetics immediately upon addition of $Si(OH)_4$. Pool levels then gradually increase (Hildebrand et al., 2007) to maintain equilibrium with the increasing demand for silica incorporation, and presumably a concurrent increase in the amount of Si-binding component occurs.

One aspect not addressed in our experiments, but dealt with in other investigations, is the role of efflux in overall transport. In the absence of extracellular $Si(OH)_4$, efflux does not occur (Sullivan, 1976). Given the high intracellular soluble Si concentrations (Martin-Jézéquel et al., 2000), lack of $Si(OH)_4$ efflux is consistent with the intracellular pool being in a different chemical form than extracellular $Si(OH)_4$ (e.g. through complexation with an organic compound). Efflux occurred only above a threshold amount of added $Si(OH)_4$ (Sullivan, 1976), consistent with efflux occurring only after surge uptake. These results suggest efflux is likely to be a contributing factor in the equilibration process between pools and incorporation (Fig. 8C).

Transition from Short-Term Nonsaturable to Long-Term Saturable Uptake Kinetics Occurred in All Diatom Species Tested

All species tested followed a similar trend toward saturation as *T. pseudonana*. The rate at which saturability was achieved varied depending on the species (Fig. 6B), with the exception of *T. weissflogii*, in which uptake approached saturability but was not achieved. At least three variables could come into play regarding how fast saturability is achieved: the rate of uptake (how fast the pools are replenished), the rate of silica incorporation (how fast the pools are depleted), and the rate of change in capacity of the pools (i.e. the amount of available binding component). A simplistic way of determining the effect of pools on saturability is to compare the ratio of cell wall silica to pools (Fig. 7), with the assumption that a higher ratio means pools would be depleted more rapidly and saturation would occur faster. Analyzing data for uptake and rate of saturation (Fig. 6) and cell wall silica to pools (Fig. 7) did not reveal any clear trends in this regard; however, three interesting observations could be made. First, the lack of saturability in *T. weissflogii* could relate to this diatom's ability to maintain an entire cell wall worth of Si in intracellular pools (Binder and Chisholm, 1980; Brzezinski and Conley, 1994). Second, in comparing the two *N. pelliculosa* species, which have similar cell sizes and shapes, *N. pelliculosa* FW had a 4.3-fold higher cell wall to pools ratio and a 2.9-fold faster rate of saturation, consistent with the pools/incorporation equilibration hypothesis. Third, there is a general correlation between cell size (data not shown) and rate to achieve saturation (Fig. 6B), suggesting cell volume or geometry may have an effect. Cell size has previously been shown to influence V_{max}, where cells with higher surface to volume ratios have a lower V_{max} (Leynaert et al., 2004). Interestingly, *C. gracilis*, which has 80% of its cell wall silica in the form of long and narrow spines (Rogerson et al., 1986), had one of the fastest saturation times (Fig. 5B), even though its cell wall to pools ratio was near the average of the species examined.

Environmental Relevance

Concentrations of $Si(OH)_4$ in most of the ocean's photic zone average 10 μmol L^{-1} (Tréguer et al., 1995). Based on our data, $Si(OH)_4$ uptake by field assemblages would mostly be directly controlled by SITs, which would minimize the associated costs of excess surge uptake and efflux. Intracellular pools should be in equilibrium with the needs for cell wall silica; thus, uptake rates could relate to incorporation rates. In coastal environments or upwelling zones, conditions favoring surge uptake could occur; for example, cells exposed to high levels of $Si(OH)_4$ would have a higher intracellular pool capacity, allowing surge uptake to occur more frequently. Certain ocean, and many freshwater, locations have $Si(OH)_4$ levels in the realm of diffusion mediated uptake. Antarctic ocean waters can contain as high as 100 μmol L^{-1} in the winter (Tréguer et al., 1995); thus, diffusion-mediated uptake could play an important role in regulating diatom growth. In addition, diatoms once continuously experienced near saturating levels of Si (approximately 2 mM; Holland, 1984), raising the intriguing possibility that SITs initially evolved as Si effluxers and then optimized uptake ability as oceanic Si levels dropped.

MATERIALS AND METHODS

Culture Conditions

Thalassiosira pseudonana Hasle et Heimdale clone 3H CCMP1335 (Provasoli-Guillard National Center for Culture of Marine Phytoplankton, Bigelow Laboratory for Ocean Sciences), *Thalassiosira weissflogii* (Grunow) Fryxell et Hasle CCMP1336, *Cylindrotheca fusiformis* Reimann et Lewin CCMP343, *Navicula pelliculosa* (Bréb.) Hilse UTEX 668 (Culture Collection of Algae at the University of Texas at Austin; a freshwater strain, referred to as *N. pelliculosa* FW in text), *N. pelliculosa* (Breb. et Kuetzing) Hilse CCMP543 (a marine strain, referred to as *N. pelliculosa* M in text), *Phaeodactylum tricornutum* Bohlin CCMP1327, *Chaetoceros gracilis* Schütt UTEX LB2658, and *Nitzschia alba* Lewin and Lewin CCMP2426 were grown in batch culture under continuous illumination with cool-white fluorescent lights at approximately 150 μmol quanta m^{-2} s^{-1} at 18°C to 20°C. *N. pelliculosa* FW was grown in freshwater tryptone medium (Reimann et al., 1966). All other diatom species were grown in artificial seawater (ASW) medium (Darley and Volcani, 1969) with biotin and vitamin B12 added to 1 ng L^{-1} or f/2 medium made with 0.2 μm filtered and autoclaved local seawater (Guillard and Ryther, 1962; Guillard, 1975).

$Si(OH)_4$ Uptake Kinetic Measurements

$Si(OH)_4$ uptake rates vary at different stages of the cell cycle (Brzezinski, 1992). In addition, Si requirements at different cell cycle stages vary depending on the species (Brzezinski et al., 1990; Martin-Jézéquel et al., 2000). Thus, to

avoid possible cell cycle and cell phasing effects, which are difficult to controllably reproduce, exponentially growing cultures in continuous light were used in all measurements. Preliminary measurements were done to determine the optimal cell concentration for each species that would result in counts significantly above background. This was 2.5×10^5 cells mL^{-1} for most species with the exception of *P. tricornutum* and *N. pelliculosa* FW, which required 2.0×10^6 cells mL^{-1}. $Si(OH)_4$ uptake was measured using the radiotracer analog of silicic acid, $^{68}Ge(OH)_4$, because it is available in high specific activity and carrier-free form (enabling short-term uptake measurements), has a relatively long half-life of 282 d, and has well-established protocols for measuring silicic acid transport in diatoms (Azam, 1974; Azam et al., 1974; Sullivan, 1976, 1977). Stock solutions containing 1.0 μCi mL^{-1} of $^{68}Ge(OH)_4$ and 10-fold concentrations of freshly made sodium silicate in 3.5% NaCl (MilliQ-treated water for *N. pelliculosa* FW) were prepared, and for a given concentration of silicate, 100 μL of ^{68}Ge:silicate stock per 1 mL of cells was assayed. For most experiments, 1, 2, 4, 8, 10, 15, 30, and 100 μmol L^{-1} final silicate concentrations were used, with duplicates being done for 8 to 30 μmol L^{-1}. Cells were harvested by centrifugation at 3,000*g* for 5 min, then washed and resuspended in Si-free medium. For all experiments, with the exception of Figure 4B, cells were maintained in Si-free medium for 5 to 10 min (referred to as short-term Si starvation) prior to measuring $Si(OH)_4$ uptake. Long-term Si starvation was done for 24 h prior to measurements (Fig. 4B). After the addition of various silicate concentrations, cells were incubated in the light and aliquots removed at different incubation times, vacuum filtered onto a Millipore Isopore 1.2-μm RTTP membrane, and washed with 5 mL of 3.5% NaCl (MilliQ-treated water for *N. pelliculosa* FW). Background was minimal with this wash treatment. Short-term uptake refers to uptake measured after 2 min; long-term uptake refers to uptake measured after 1 to 3 h. For measurement of background, 1 mL of cells was added to separate tubes containing 100 μL of ^{68}Ge:silicate and immediately pipetted onto a Millipore membrane and washed. This manipulation took 8 to 10 s, so cellular binding and some uptake may have occurred during this time, but because this would be minimal and a consistent procedure was used in all experiments, subtraction of 0 min from the longer time points was used to calculate net uptake for those time points. Filters were counted either dry using a LKB Wallac 1282 Compugamma CS Universal gamma counter (Perkin-Elmer) or in 10 mL of water by Cherenkov counting in a Beckmann LSC6000TA scintillation counter (Beckman Coulter). Counts per minute were converted to femtomoles per cell per hour, taking into account counting efficiency, dilution effects, and radioactive decay. Data obtained using this method are referred to as $Si(OH)_4$ uptake. Data were analyzed using the software program GraphPad Prism 4. Uptake rates were expressed in hours even when short-term uptake was measured to more easily compare data between experiments and with past studies.

Inhibition of Uptake by $Ge(OH)_4$

Unlabeled $Ge(OH)_4$ was used as a competitive inhibitor of $Si(OH)_4$ uptake (Azam et al., 1974). Short-term (2 min) $Si(OH)_4$ uptake was measured in *T. pseudonana* as described above except that increasing concentrations of a constant ratio of $Si(OH)_4$:$Ge(OH)_4$ (1:0.33) were added.

Effect of Zinc Chelators on Si Uptake

A control experiment was done to test the effect of the membrane-impermeable divalent cation chelator Na_2EDTA and membrane-permeable zinc-specific chelator TPEN (Hitomi et al., 2001) on growth of *T. pseudonana*. A stock solution of 25 mmol L^{-1} Na_2EDTA was made in water and of TPEN in 100% dimethyl sulfoxide (DMSO). Five-milliliter cultures of *T. pseudonana* were established with 1×10^5 cells mL^{-1} in the presence of Na_2EDTA and TPEN concentrations ranging from 0 to 1 mmol L^{-1}. Culture cell density was monitored after 8 d. For both chelators, no growth occurred above a concentration of 25 μmol L^{-1}, and equivalent volumes of DMSO alone did not inhibit growth. To confirm the specificity of TPEN for zinc, cultures were established at 2×10^5 cells mL^{-1} in the presence of 50 μmol L^{-1} TPEN and increasing concentrations (50, 100, or 200 μmol L^{-1}) of $CaCl_2$, $FeSO_4$, or $ZnCl_2$. After 4 d, cell density was determined. To monitor the effect of the chelators on $Si(OH)_4$ uptake, exponentially growing cultures of *T. pseudonana* were harvested by centrifugation and washed in Si-free ASW. Cells were resuspended in Si-free ASW at a density of 2.5×10^5 mL^{-1}. Chelators were added to separate tubes at a final concentration of 50 μmol L^{-1}. Control tubes had no addition or addition of an equivalent amount of DMSO as in the TPEN addition. These were allowed to incubate for 5 min after which 15 μmol L^{-1} $^{68}Ge(OH)_4$ was added. Uptake was measured after 30 min as already described, with a 0-min time point used to calculate background.

Measurements of Cell Wall Silica and Intracellular Soluble Si Pools

Aliquots of cells (approximately 1.3×10^7) during exponential growth were harvested in 14-mL Falcon 1029 polypropylene tubes and pelleted at 16,500*g* in an HB-4 rotor (Sorvall, Thermo Electron) for 4 min. Cells were washed in Si-free medium, repelleted, and stored at −20°C. Intracellular soluble Si pool levels were measured using the boiling water method of Sullivan (1979). Frozen cells were resuspended in 1 mL of MilliQ-treated water, boiled for 10 min, cooled, and then centrifuged for 5 min at 16,500*g* in an HB-4 rotor. Triplicate samples of supernatant were assayed for intracellular Si. Cell wall silica was determined by resuspending the boiled cell pellet in 4 mL of 0.5 N NaOH (made from solid NaOH dissolved in MilliQ water) and placing the tube in a boiling water bath for 15 min. After cooling, samples were neutralized with 2 mL of 1 N HCl and then centrifuged for 5 min at 16,500*g* in an HB-4 rotor. Triplicate samples of supernatant were assayed to measure cell wall silica. Silicic acid concentrations were measured using the silicomolybdate assay (Strickland and Parsons, 1968). The standard was sodium hexafluorosilicate (Sigma), used in a range of 0 to 50 μmol L^{-1}.

ACKNOWLEDGMENTS

We thank Michael I. Latz and Bradley M. Tebo for use of lab space and equipment. We appreciate both encouraging words and helpful technical advice from Mark A. Brzezinski. We also thank Assaf Vardi for comments and suggestions on the manuscript and Adam B. Kustka for discussions about zinc. *N. pelliculosa* (Breb. et Kuetzing) Hilse CCMP543 was provided as part of a collaborative project with S. Hazelaar and W.W.C. Gieskes.

Received August 8, 2007; accepted December 20, 2007; published December 27, 2007.

LITERATURE CITED

Azam F (1974) Silicic acid uptake in diatoms studied with [^{68}Ge]germanic acid as a tracer. Planta **121:** 205–212

Azam F, Hemmsingsen BB, Volcani BE (1974) Role of silicon in diatom metabolism. V. Silicic acid transport and metabolism in the heterotrophic diatom *Nitzschia alba*. Arch Microbiol **97:** 103–114

Azam F, Volcani B (1974) Role of silicon in diatom metabolism. VI. Active transport of germanic acid in the heterotrophic diatom *Nitzschia alba*. Arch Microbiol **101:** 1–8

Bhattacharyya P, Volcani BE (1983) Isolation of silicate ionophores from the apochlorotic diatom *Nitzschia alba*. Biochem Biophys Res Commun **114:** 365–372

Binder BJ, Chisholm SW (1980) Changes in the soluble silicon pool size in the marine diatom *Thalassiosira fluviatilis*. Marine Biology Letters **1:** 205–212

Brzezinski MA (1992) Cell-cycle effects on the kinetics of silicic acid uptake and resource competition among diatoms. J Plankton Res **14:** 1511–1539

Brzezinski MA, Conley DJ (1994) Silicon deposition during the cell cycle of *Thalassiosira weissflogii* (Bacillariophyceae) determined using dual rhodamine 123 and propidium iodide staining. J Phycol **30:** 45–55

Brzezinski MA, Olson RJ, Chisholm SW (1990) Silicon availability and cell cycle progression in marine diatoms. Mar Ecol Prog Ser **67:** 83–96

Collos Y, Siddiai MY, Wang MY, Glass ADM, Harrison PJ (1992) Nitrate uptake kinetics by two marine diatoms using the radiotracer ^{13}N. J Exp Mar Biol Ecol **163:** 251–260

Collos Y, Vaquer A, Bibent B, Slawyk G, Garcia N, Souchu P (1997) Variability in nitrate uptake kinetics of phytoplankton communities in a Mediterranean coastal lagoon. Estuar Coast Shelf Sci **44:** 369–375

Conway HL, Harrison PJ (1977) Marine diatoms grown in chemostats under silicate or ammonium limitations IV. Transient response of *Chaetoceros debilis*, *Skeletonema costatum*, and *Thalassiosira gravida* to a single addition of the limiting nutrient. Mar Biol **43:** 33–43

Conway HL, Harrison PJ, Davis CO (1976) Marine diatoms grown in chemostats under silicate or ammonium limitation. II. Transient re-

sponse of *Skeletonema costatum* to a single addition of the limiting nutrient. Mar Biol **35:** 187–199

Darley WM, Volcani BE (1969) Role of silicon in diatom metabolism: a silicon requirement for deoxyribonucleic acid synthesis in the diatom *Cylindrotheca fusiformis* Reimann and Lewin. Exp Cell Res **58:** 334–342

Del Amo Y, Brzezinski MA (1999) The chemical form of dissolved Si taken up by marine diatoms. J Phycol **35:** 1162–1170

Eppley RW, Rogers JN, McCarthy JJ (1969) Half-saturation constants for uptake of nitrate and ammonium by marine phytoplankton. Limnol Oceanogr **14:** 912–920

Grachev MA, Denikina NN, Belikov SI, Likhoshvai EV, Usol'tseva MV, Tikhonova IV, Adel'shin RV, Kler SA, Sherbakova TA (2002) Elements of the active center of silicon transporters in diatoms. Mol Biol (Mosk) **36:** 534–536

Guillard RR, Ryther JH (1962) Studies of marine planktonic diatoms. I. *Cyclotella nana* Hustedt and *Detonula confervacea* Cleve. Can J Microbiol **8:** 229–239

Guillard RRL (1975) Culture of phytoplankton for feed marine invertebrates. *In* WL Smith, MH Chanley, eds, Culture of Marine Invertebrate Animals. Plenum Press, New York, pp 29–60

Hamill S, Cloherty EK, Carruthers A (1999) The human erythrocyte sugar transporter presents two sugar import sites. Biochemistry **38:** 16974–16983

Harrison PJ, Parslow JS, Conway HL (1989) Determination of nutrient uptake kinetic parameters: a comparison of methods. Mar Ecol Prog Ser **52:** 301–312

Higgins CF, Linton KJ (2004) The ATP switch model for ABC transporters. Nat Struct Mol Biol **11:** 918–926

Hildebrand M (2000) Silicic acid transport and its control during cell wall silicification in diatoms. *In* E Bäuerlein, ed, Biomineralization: From Biology to Biotechnology and Medical Applications. Wiley-VCH, Weinheim, Germany, pp 171–188

Hildebrand M, Dahlin K, Volcani BE (1998) Characterization of a silicon transporter gene family in *Cylindrotheca fusiformis*: sequences, expression analysis, and identification of homologs in other diatoms. Mol Gen Genet **260:** 480–486

Hildebrand M, Frigeri LG, Davis AK (2007) Synchronized growth of *Thalassiosira pseudonana* (Bacillariophyceae) provides novel insights into cell wall synthesis processes in relation to the cell cycle. J Phycol **43:** 730–740

Hildebrand M, Volcani BE, Gassmann W, Schroeder JI (1997) A gene family of silicon transporters. Nature **385:** 688–689

Hildebrand M, Wetherbee R (2003) Components and control of silicification in diatoms. *In* WEG Muller, ed, Progress in Molecular and Subcellular Biology, Vol 33. Springer-Verlag, Berlin, pp 11–57

Hitomi Y, Outten CE, O'Halloran TV (2001) Extreme zinc-binding thermodynamics of the metal sensor/regulator protein, ZntR. J Am Chem Soc **123:** 8614–8615

Holland HD (1984) The Chemical Evolution of the Atmosphere and Oceans. Princeton University Press, Princeton

Iler RK (1979) The Chemistry of Silica: Solubility, Polymerization, Colloid and Surface Properties, and Biochemistry. John Wiley & Sons, New York

Johnson RN, Volcani BE (1978) The uptake of silicic acid by rat liver mitochondria. Biochem J **172:** 557–568

Koshland DE Jr, Németh G, Filmer D (1966) Comparison of experimental binding data and theoretical models in proteins containing subunits. Biochemistry **5:** 365–385

Leynaert A, Bucciarelli E, Claquin P, Dugdale RC, Martin-Jézéquel V, Pondaven P, Ragueneau O (2004) Effect of iron deficiency on diatom cell size and silicic acid uptake kinetics. Limnol Oceanogr **49:** 1134–1143

Likoshway YV, Masyukova YA, Sherbakova TA, Petrova DP, Grachev MA (2006) Detection of the gene responsible for silicic acid transport in chrysophycean algae. Dokl Akad Nauk SSSR **408:** 845–849

Lomas MW, Glibert PM (1999) Temperature regulation of nitrate uptake: a novel hypothesis about nitrate uptake and reduction in cool-water diatoms. Limnol Oceanogr **44:** 556–572

Ma JF, Mitani N, Nagao S, Konishi S, Tamai K, Iwashita T, Yano M (2004) Characterization of the silicon uptake system and molecular mapping of the silicon transporter gene in rice. Plant Physiol **136:** 3284–3289

Ma JF, Yamaji N, Mitani N, Tamai K, Konishi S, Fujiwara T, Katsuhara M, Yano M (2007) An efflux transporter of silicon in rice. Nature **448:** 209–212

Martin-Jézéquel V, Hildebrand M, Brzezinski MA (2000) Silicon metabolism in diatoms: implications for growth. J Phycol **36:** 821–840

McCarthy JJ (1981) The kinetics of nutrient utilization. Can Bull Fish Aquat Sci **210:** 211–233

Milligan A, Varela DE, Brzezinski MA, Morel FMM (2004) Dynamics of silicon metabolism and silicon isotopic discrimination in a marine diatom as a function of *p*CO2. Limnol Oceanogr **49:** 322–329

Nelson DM, Goering JJ, Kilham SS, Guillard RRL (1976) Kinetics of silicic acid uptake and rates of silica dissolution in the marine diatom *Thalassiosira pseudonana*. J Phycol **12:** 246–252

Paasche E (1973a) Silicon and the ecology of marine plankton diatoms. I. *Thalassiosira pseudonana* (*Cyclotella nana*) grown in a chemostat with silicate as limiting nutrient. Mar Biol **19:** 117–126

Paasche E (1973b) Silicon and the ecology of marine plankton diatoms. II. Silicate-uptake kinetics in five diatom species. Mar Biol **19:** 262–269

Reidel GF, Nelson DM (1985) Silicon uptake by algae with no known Si requirement. II. Strong pH dependence of uptake kinetic parameters in *Phaeodactylum tricornutum* (Bacillariophyceae). J Phycol **21:** 168–171

Reimann BEF, Lewin JC, Volcani BE (1966) Studies on the biochemistry and fine structure of silica shell formation in diatoms. II. The structure of the cell wall of *Navicula pelliculosa* (Breb.) Hilse. J Phycol **2:** 74–84

Rogerson A, DeFreitas ASW, McInnes AG (1986) Growth rates and ultrastructure of siliceous setae of *Chaetoceros gracilis* (Bacillariophyceae). J Phycol **22:** 56–62

Rogerson A, DeFreitas ASW, McInnes AG (1987) Cytoplasmic silicon in the centric diatom *Thalassiosira pseudonana* by electron spectroscopic imaging. Can J Microbiol **33:** 128–131

Rueter JG Jr, Morel FMM (1981) The interaction between zinc deficiency and copper toxicity as it affects the silicic acid uptake mechanisms in *Thalassiosira pseudonana*. Limnol Oceanogr **26:** 67–73

Sherbakova TA, Masyukova Y, Safonova T, Petrova D, Vereshagin A, Minaeva T, Adelshin R, Triboy T, Stonik I, Aizdaitcher N, et al (2005) Conserved motif CMLD in silicic acid transport proteins of diatoms. Mol Biol (Mosk) **39:** 269–280

Strickland JDH, Parsons TR (1968) A practical handbook of sea water analysis. Bull Fish Res Board Can **167:** 1–311

Suana ZE, Ambudkar SV (2007) About a switch: how P-glycoprotein (ABCB1) harnesses the energy of ATP binding and hydolysis to do mechanical work. Mol Cancer Ther **6:** 13–23

Sullivan CW (1976) Diatom mineralization of silicic-acid. I. Si(OH)4 transport characteristics in *Navicula pelliculosa*. J Phycol **12:** 390–396

Sullivan CW (1977) Diatom mineralization of silicic acid. II. Regulation of $Si(OH)_4$ transport rates during the cell cycle of *Navicula pelliculosa*. J Phycol **13:** 86–91

Sullivan CW (1979) Diatom mineralization of silicic acid. IV. Kinetics of soluble Si pool formation in exponentially growing synchronized cultures of *Navicula pelliculosa*. J Phycol **15:** 210–216

Thamatrakoln K, Alverson AJ, Hildebrand M (2006) Comparative sequence analysis of diatom silicon transporters: towards a mechanistic model of silicon transport. J Phycol **42:** 822–834

Tréguer P, Nelson DM, Van Bennekom AJ, DeMaster DJ, Leynaert A, Queguiner B (1995) The silica balance in the world ocean: a reestimate. Science **268:** 375–379

Vrieling EG, Sun Q, Tian M, Kooyman PJ, Gieskes WWC, van Santen RA, Sommerdijk NAJM (2007) Salinity-dependent diatom biosilicification implies an important role of external ionic strength. Proc Natl Acad Sci USA **104:** 10441–10446

Watt DA, Armory AM, Cresswell CF (1992) Effect of nitrogen supply on the kinetics and regulation of nitrate assimilation in *Chlamydomonas reihnardtii* Dangeard. J Exp Bot **43:** 605–615

Wheeler PA, Glibert PM, McCarthy JJ (1982) Ammonium uptake and incorporation by Chesapeake Bay phytoplankton: short-term uptake kinetics. Limnol Oceanogr **27:** 1113–1128

Zelcer N, Huisman MT, Reid G, Wielinga P, Breedveld P, Kuil A, Knipscheer P, Schellens JHM, Schinkel AH, Borst P (2003) Evidence of two interacting lignad binding sites in human multidrug resistance protein 2 (ATP binding cassette C2). J Biol Chem **276:** 23538–23544